Radius Estimate by Dynamic Data Acquisition

Sabag, Matthew

Section 3458 06/01/2026

***Abstract*—The objective of this experiment is to evaluate and analyze different methods of determining the radius of curvature for a laboratory stool footrest. To complete this experiment, a quarter Wheatstone Bridge (WSB) paired with a feeler gauge and a strain gauge are connected to a 14-bit analog-to-digital converter (ADC) to acquire voltage signals. Using three separate sample windows to mitigate saturation, strain is computed through a direct bridge voltage (V_g) and an amplified voltage (V_{amp}, gain = 900). With these recorded voltages, the radii can be derived from mathematical theory. A third radius estimation was acquired using a flexible measuring tape along the circumference of the footrest. The catalogued radii are 256.2 ± 37.0 mm (V_g), 252.8 ± 3.0 mm (V_{amp}), and 254.17 ± 0.080 mm (tape measure). The three radius values agreed with each other, being only a few millimeters apart and proving that strain-based radius estimation is viable, precise, and accurate.**

***Index Terms*—Analog-to-digital converter, feeler gauge, quarter Wheatstone bridge, radius of curvature, sample window, saturation, strain gauge.**

I. Introduction

DYNAMIC data acquisition can be directly related to radius estimation, the primary objective of this experiment. Exact physical properties of curved structural components are a common challenge in engineering design, especially when a component's radius directly impacts how it handles stress under a load. While standard manual tools like flexible tape measures can give a quick, rough measurement, modern engineering relies heavily on digital readings from a Data Acquisition device (DAQ) for automatic readings. Converting physical measurements into digital information introduces several challenges, making the transducer unable to transmit data exactly one to one. Issues like electrical noise, limits in signal resolution, and saturation in the software can easily distort the data if the equipment is not set up correctly. Understanding how digital hardware processes analog input is essential for getting accurate digitized structural readings.

In this lab, an elastic steel feeler gauge was wrapped tightly around a curved surface, forcing the material to deflect and experience a surface strain relative to its distance from its neutral axis. A strain gauge was bonded to the feeler gauge to capture this small movement. The gauges were wired into a WSB to convert the mechanical resistance changes into small changes in voltage. Because these raw signals (V_g) are usually too small to analyze accurately, an inline amplifier was used to scale the signal up (V_{amp}). This amplified signal was then sent to a 14-bit ADC monitored through the LabVIEW software. To prevent the voltage from clipping, or cutting off, while still maintaining good resolution, the software data collection windows had to be carefully adjusted based on the signal size.

To relate the measured readings of the voltage changes back to the structural properties of the footrest, specific mathematical equations were applied and manipulated within the software. The fundamental relationship used to convert the recorded electrical signals into mechanical strain (ε) relied on the WSB equation (1), where V_g represents the differential bridge voltage, V_s is the source excitation voltage, G_f is the factory-defined gauge factor of the strain gauge, V_{amp} is the amplified voltage, and $gain$ represents the gained value for amplification. When considering the amplified voltage, the equation was modified to account for the inline signal scaling by introducing the amplifier gain into the denominator.

$$\varepsilon = \frac{4\Delta V_g}{V_s G_f} = \frac{4\Delta V_{amp}}{gain V_s G_f} \tag{1}$$

Before converting the electronic signals into strain values, the raw voltage readings had to be corrected from any initial offset. A tare operation was performed to record the baseline state of the resting circuit, yielding a fixed reference value $V_{x,Tare}$ for both the raw voltage (2) and amplified voltage (3) readings. The true change in voltage (ΔV_x) caused purely by the mechanical bending of the feeler gauge was then isolated by subtracting this baseline offset from the active voltage readings (V_x). This tare operation essentially zeroed out any preexisting error within the feeler gauge.

$$\Delta V_g = V_g - V_{g,Tare} \tag{2}$$

$$\Delta V_{amp} = V_{amp} - V_{amp,Tare} \tag{3}$$

The strain gauge, which functioned as a transducer that converted mechanical movement into resistance changes, was bonded directly to the surface of the feeler gauge. This flexible strip of metal was used to measure the bending and directly convert the reading into measurable strain. To capture these microscopic changes, the strain gauge was wired into a Printed Circuit Board (PCB). The PCB acted as the motherboard that connects the WSB to the rest of the circuit. This electrical network used two parallel voltage dividers to transform the small variations in component resistance into a measurable differential output voltage, represented in Fig. 1.

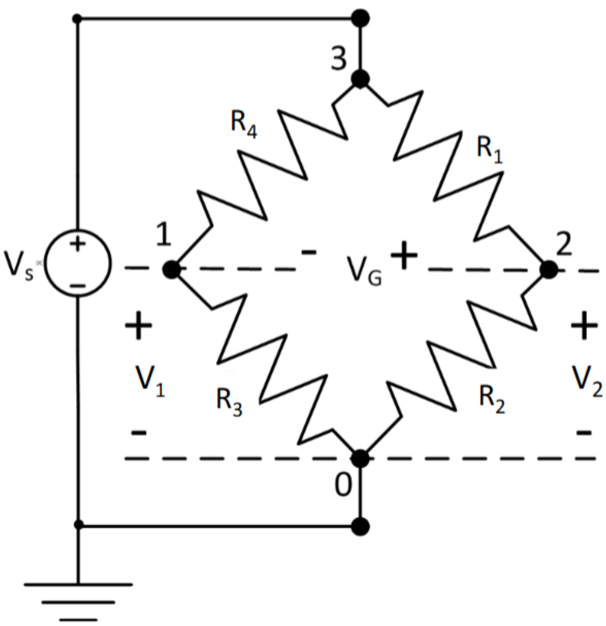

Fig. 1. Wheatstone Bridge diagram, used to understand how the circuit balances resistance values with great precision. One resistor acts as an active strain gauge and the remainder act as dummy resistors [2].

To establish how software settings affected data precision, the resolution limit of the DAQ was evaluated. The continuous voltage ranges were converted into discrete digital steps by a 14-bit ADC, where the smallest detectable change in voltage was determined by the software sample window bounds (4).

$$Resolution = \frac{V_{Max} - V_{Min}}{2^n - 1} \tag{4}$$

Here, V_{Max} and V_{Min} represented the upper and lower voltage bounds of the selected sample window, and n represented the 14-bit resolution depth of the hardware. This formula showed that narrowing the span between the maximum and minimum voltage bounds directly increased the measurement precision. This is done by reducing the size of each discrete digital step since there is a set number of digital steps as per the denominator, $n = 14$. With this, the smaller the difference, the smaller size of steps that were taken, and therefore a greater resolution. This is the case provided that the signal readings did not exceed the window bounds and saturate, rendering the reading insufficient and the sample window too small.

To transition from the electrical strain readings to a physical dimension like the radius of the footrest, we rely on relevant mechanics-of-materials relationships (5).

$$\varepsilon = \frac{y}{r} \tag{5}$$

In this relationship, ε represents the experimental strain experienced by the material, while r is the radius extending directly to the structural neutral axis of our bending setup. The variable y denotes the distance from that neutral axis to the outer surface where the strain gauge is attached, seen in Fig. 2.

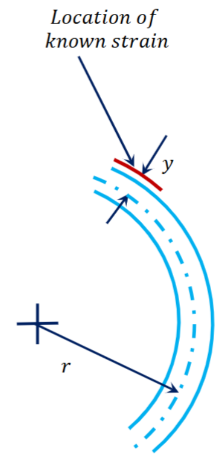

Fig. 2. Strain radial distance, used to visualize how to determine the distance strain is applied from the neutral axis while incorporating the distance from the neutral axis to the outer surface, y, to accurately represent the strain [2].

To find y precisely, we must account for both the thickness of the feeler gauge and the strain gauge itself. To do this, we used the equation (6) to determine the distance from the neutral axis to the outer surface. Here, d stands for the specific thickness of the strain gauge material, and t represents the thickness of the feeler gauge underneath, which splits perfectly in half to locate the center of bending.

$$y = d + \frac{t}{2} \tag{6}$$

Finally, because the strain gauge is layered on top of the feeler gauge rather than flush against the footrest, the actual radius of the neutral axis (r) overestimates the physical object. To correct for this and isolate the true inner radius of the stool's footrest (r_i), we subtract half of the feeler gauge thickness from our neutral axis calculation, giving us the appropriate radius (7).

$$r_i = r - \frac{t}{2} \tag{7}$$

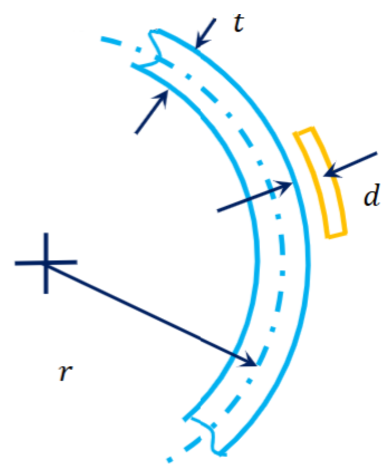

Fig. 3. Updated strain radial distance, used to visualize how to determine the distance strain is applied from the neutral axis while incorporating the thickness of the feeler gauge, t, and the thickness of the strain gauge, d, to accurately represent the strain [2].

We can update this equation by substituting in r into the equation to get the final expanded equation to use (8). This complete equation accurately represents the radius defined by the thicknesses of the feeler and strain gauges, as well as the calculated strain from the measured voltages.

$$r_i = \frac{d + {}^{t}/_{2}}{\varepsilon} - \frac{t}{2} \tag{8}$$

The final portion involving the acquisition of radial values is the manual measurement of the footrest using a tape measure, a direct baseline measurement to compare against our strain-based approximations. To get a direct physical estimate of the radius, we relate the circumference of the footrest to its radius using the basic circumference equation (9). The circumference is denoted by C and the directly measured radius is denoted by r. This serves as our control value, allowing us to see how accurate our digital data acquisition and strain calculations are.

$$r = \frac{C}{2\pi} \tag{9}$$

II. PROCEDURE

A. Materials

The experimental setup required data acquisition hardware, circuit components, and manual measuring tools. A DAQ was necessary for collection. A USB-C to -C cable connected the DAQ to a WSB PCB to capture electrical resistance variations. Eight electrical wires were connected between the DAQ terminal ports and the bridge using a small flathead screwdriver to secure the terminal connections [4]. The deformation sensor consisted of a foil strain gauge permanently adhered to a flexible steel feeler gauge. Masking tape was utilized to temporarily secure the feeler gauge assembly tightly against the stool footrest during data collection, and a measuring tape was used to manually measure the circumference of the laboratory stool footrest. The measuring tape was wrapped firmly as well.

B. Prelab Preparations

Before collecting physical data, the digital software configuration was established. A custom virtual instrument script (VI) was built within the LabVIEW software following the configuration instructions provided [3]. Within the primary program, a custom radius calculation sub-virtual instrument (sub-VI) was created to automatically process the data and ultimately served to instantly convert measured voltages into radius estimates based on the given equations mapped within the sub-VI. This was accomplished with given instructions [3].

C. Sample Window Resolution & Saturation

To optimize the signal quality before taking final measurements for radius estimation, each sample window was isolated and tested to analyze how software limitations influence digital resolution and signal saturation. The input signal was passed through the 14-bit ADC while individually cycling through five discrete sample windows: ±0.64 V, ±1.28 V, ±2.56 V, ±5.12 V, and ±10.24 V. The adjusted sample windows were ACH 0-2 as channel three was unwired and unused [1]. By evaluating the balance between maximum voltage precision and clipping behavior, the optimal window sizes were identified for the raw and amplified channels. Ideally, the smallest sample window size that does not saturate values would be employed. This step ensured that the final data collected would optimize signal-to-noise ratios without hitting the limits of the hardware and yield unusable data.

D. Radius of Curvature Estimate

The final phase of the experiment focused on proper data collection. With the feeler gauge pressed flat against a table surface in an undeformed state, a software tare was conducted to zero out any offset on both the unamplified raw bridge voltage (V_g) and the amplified voltage (V_{amp}) channels. The feeler gauge was then wrapped along the curve of the stool footrest and locked in place using masking tape, forcing the strain gauge to experience steady deflection, depicted in Fig. 4. The resulting voltages were saved through LabVIEW and transferred to an organized excel sheet. Finally, a manual measurement was acquired by wrapping the flexible measuring tape around the outer circumference of the footrest to calculate a baseline radius, allowing for a direct comparison of accuracy and uncertainty between the digital transducer data and the manual physical measurement.

Fig. 4. The experiment apparatus of the feeler and strain gauges tightly wrapped around the laboratory stool footrest using masking tape [2].

III. RESULTS

The first section of the experiment determined data acquisition stability across five distinct sample windows to ensure the lowest unsaturated window was used when collecting data (Table I). As per (4), the smaller the sample window, the greater the resolution. This step was necessary to avoid inaccurate readings for the later radius estimation when using the experiment apparatus on the laboratory stool footrest.

TABLE I
RAW VOLTAGES & SD FOR SAMPLE WINDOWS

Sample Window (V)	Resolution (V)	Mean V_s (V)	σ, V_s (V)	Mean V_g (V)	σ, V_g (V)	Mean V_{amp} (V)	σ, V_{amp} (V)
±0.64	0.000078	0.639922*	0	0.000695	0.000057	-0.00239	0.004106
±1.28	0.00016	1.279844*	0	0.000596	0.000067	-0.006764	0.004179
±2.56	0.00031	2.498644	0.000152	0.000319	0.000044	-0.00746	0.004083
±5.12	0.00063	2.497801	0.000079	0*	0	-0.010616	0.004009
±10.24	0.0013	2.49719	0.000625	0*	0	-0.011771	0.004251

*Saturated voltage readings were indicated by a standard deviation of zero and signify the sample window used was too small for an accurate measurement.

The data in this table was collected as instructed [1] where each used channel was set to the listed sample window size and the feeler gauge was placed on a flat surface. Each measurement was saved as a single datapoint of 2500 samples, and this was repeated for all five sample windows.

Each sample window had a respective strain for V_{amp} and V_g. The calculated strain values from both the raw and amplified signals varied significantly as the amplified signals ranged from -0.000008 to -0.000011 and the raw signals ranged from -0.00055 to -0.00103 (Table II). The difference in order of magnitude highlights how scaling the raw voltage signals change the resulting strain values before they are used to estimate the final radius (8).

TABLE II
RAW STRAIN VALUES FOR SAMPLE WINDOWS

Sample Window (V)	ε, V_{amp}	ε, V_g
±0.64	-0.00103	-0.000008
±1.28	-0.000663	-0.000011
±2.56	-0.00055	-0.000006
±5.12	-0.000797	-0.000009
±10.24	-0.000797	-0.00001

Using the collected data from Table I and Table II, the appropriate sample window sizes for channels 0-2 were determined to be ± 2.56 V, ± 0.64 V, and ± 2.56 V, respectively. Once this step has been implemented, the voltages must be tared (2) to remove initial offset in the readings (Table III).

TABLE III
TARE VALUES & FOOTREST VOLTAGES

Variable	Voltage (V)	SD (V)
$V_{g,Tare}$	0.000823 ± 0.00011	0.000056
$V_{amp,Tare}$	-0.106554 ± 0.00875	0.004376
ΔV_g	0.001127 ± 0.00016	-
ΔV_{amp}	−1.01729 ± 0.0120	-
V_g	0.00195 ± 0.0001	0.000059
V_{amp}	-1.123843 ± 0.00817	0.004085

Table IV shows each relevant variable with its associated final radius value and uncertainty after the tare operation.

TABLE IV
FINAL RADII ESTIMATION & UNCERTAINTY

Variable	Magnitude and Uncertainty*
ε, V_g	-0.000911 ± 0.00013
ε, V_{amp}	0.000897 ± 0.00001
C	1597 ± 0.5
r_i (V_g)	256.2 ± 37.0
r_i (V_{amp})	252.8 ± 3.0
r_i (C)	254.17 ± 0.080

*Strain, ε, is unitless but reported as mm/mm for good practice. All other reported values, both circumferential and radial, are measured in millimeters.

IV. Discussion

A. Context, Objectives, & Results

This experiment set out to evaluate different methods of data acquisition using distinct configurations. These parameters affected the precision of strain gauge measurements when estimating the dimensions of a laboratory footrest. By analyzing subtle changes in resistance from a feeler gauge using a Wheatstone Bridge connected to a data acquisition device, we mapped raw and amplified voltage changes. These voltage changes can be manipulated to derive strain and radius values. The calculated radii and their respective uncertainties are 256.2 ± 37.0 mm (V_g), 252.8 ± 3.0 mm (V_{amp}), and 254.17 ± 0.080 mm (tape measure). The amplified channel ultimately yielded a highly accurate radius estimation that aligned closely with our manual baseline utilizing a tape measure.

B. Interpretation & Analysis

The amplified voltage behaved as expected, ensuring the highest resolution with the smallest sample window. This yielded a much narrower range of uncertainty (± 3.0 mm) compared to the raw voltage (± 37.0 mm). Our quantitative selection of sample window sizes relied directly on optimizing signal standard deviation while maximizing resolution. Saturated readings occurred when a voltage channel hits its physical hardware limit and the signal essentially flatlines. This drove the standard deviation to zero, behaving as a perfectly precise reading but this indicated a loss of data within the LabVIEW processes and yielded insufficient readings. Channels 0-2 correspond to V_s, V_g, and V_{amp}, respectively, and based on Table I, the appropriate DAQ input voltage ranges to allocate to these channels were ± 2.56 V, ± 0.64 V, and ± 2.56 V. This configuration ensured that the smallest possible window did not saturate the voltage values, optimizing the resolution and minimizing the step size per bit within the DAQ.

C. Uncertainty & Limitations

To measure the reliability of the data collected and the subsequent calculations, these values were integrated together via a Root-Sum-Square (RSS) error propagation analysis to obtain the final error propagated to our calculated radius values. The largest contributor to our uncertainty was the unamplified bridge voltage (V_g), where microscopic fluctuations were then amplified when inverted in the denominator of the radius equation (1, 8). This caused the unamplified radius estimate to fall within a wide ± 37.0 mm range. Conversely, utilizing the amplified channel (V_{amp}) drastically reduced error contribution, limiting the inner radius range to a narrow ± 3.0 mm. These results indicate an agreement of the true radius of the stool footrest, as their ranges overlap, alongside a strong concurrence with the 95% confidence interval. The DAQ system used in this experiment catalogued 2500 samples when considering statistical limitations. This implies that statistically calculated uncertainties were twice the standard deviation of the sample. In terms of experimental scope, these findings do not apply universally to every engineering system. They are limited to low strain, small-scale setups that experience elastic deformation (e.g. the thin, flexible feeler gauge of this experiment). Random error contributors and external factors such as manual tape-measure placement or variations in feeler gauge alignment around the footrest create discrepancy that math alone is unable to account for, meaning high-precision applications would require more secure placement and instruments of greater precision as well.

V. Conclusion

This experiment successfully demonstrated the efficacy of distinct data acquisition configurations and signal amplification to estimate a structural dimension. This was done by measuring microscopic voltage fluctuations and transforming those values into measurable strains. From strain, we can directly measure radius with known thicknesses of each gauge. Using the direct voltage (V_g), the radius was evaluated to be 256.2 ± 37.0 mm. Similarly, the amplified voltage (V_{amp}) was determined to be 252.8 ± 3.0 mm. The control radius measured manually with a tape measure was recorded as 254.17 ± 0.080 mm. These results demonstrate the viability of strain-based radius estimation and the potential value this technology can bring to fields like structural integrity and experimentation. To build on this performance in future efforts, implementing a rigid fixture, such as a dimensionally sound 3D-printed mount to hold the feeler gauge against the structure in question would eliminate manual alignment instability. Integrating a higher-bit ADC would help push step-size resolution limitations and exponentially decrease the uncertainty. The collection of more data can also yield more precise results that can be interpreted considering the 95% confidence interval, aiding with the determination of accuracy and the meaning of uncertainty.

Appendix

A. Given and Statistical Uncertainties

The following values in Table V were provided by the manufacturer or acquired by rule of thumb [1]. These values are necessary as input into the LabVIEW virtual instrument. Although π is a defined constant, its significant figures and uncertainty play a role in the propagated uncertainty.

TABLE V
VARIABLES WITH GIVEN UNCERTAINTIES

Variable	Symbol	Value and Uncertainty	Source
t	μ_t	0.40 ± 0.015 mm	Given
d	μ_d	0.030 ± 0.02 mm	Given
G_f	μ_{G_f}	2 ± 0.01*	Manufacturer
Gain	μ_{Gain}	900 ± 4.5*	Manufacturer
C	μ_C	1597 ± 0.5 mm	Rule of Thumb
π	μ_π	12 Digits*	Rule of Thumb

*Values such as G_f, Gain, and π are considered unitless.

When considering the measured voltages displayed in Table VI, the number of samples, N, is 2500. These statistical uncertainties rely on the quantity of data points to utilize the 95% confidence interval.

TABLE VI
VARIABLES & MEASURED VOLTAGES

Variable	Voltage (V)	SD (V)
$V_{g,Tare}$	0.000823 ± 0.00011	0.000056
$V_{amp,Tare}$	-0.106554 ± 0.00875	0.004376
V_s	2.498661 ± 0.00029	0.000147
V_g	0.00195 ± 0.0001	0.000059
V_{amp}	-1.123843 ± 0.00817	0.004085

B. RSS Propagation

The differential voltage uncertainty was taken into consideration when using the measured voltages and tare voltage values (10, 11).

$$\mu_{\Delta V_g}^2 = \left(\frac{\partial \Delta V_g}{\partial V_g}\mu_{V_g}\right)^2 + \left(\frac{\partial \mu_{\Delta V_g}}{\partial \mu_{V_{g,Tare}}}\mu_{V_{g,Tare}}\right)^2 \quad (10)$$

$$\mu_{\Delta V_{amp}}^2 = \left(\frac{\partial \Delta V_{amp}}{\partial V_{amp}}\mu_{V_{amp}}\right)^2 + \left(\frac{\partial \mu_{\Delta V_{amp}}}{\partial \mu_{V_{amp,Tare}}}\mu_{V_{amp,Tare}}\right) \quad (11)$$

In Table IV, the uncertainty of both strain values was calculated via RSS Propagation (12, 13).

$$\mu_{\varepsilon_{V_g}}^2 = \left(\frac{\partial \varepsilon}{\partial \Delta V_g}\mu_{\Delta V_g}\right)^2 + \left(\frac{\partial \varepsilon}{\partial G_f}\mu_{G_f}\right)^2 + \left(\frac{\partial \varepsilon}{\partial V_s}\mu_{V_s}\right)^2 \quad (12)$$

$$\mu_{\varepsilon_{V_{amp}}}^2 = \left(\frac{\partial \varepsilon}{\partial \Delta V_{amp}}\mu_{\Delta V_{amp}}\right)^2 + \left(\frac{\partial \varepsilon}{\partial gain}\mu_{gain}\right)^2 + \left(\frac{\partial \varepsilon}{\partial V_s}\mu_{V_s}\right)^2 + \left(\frac{\partial \varepsilon}{\partial G_f}\mu_{G_f}\right)^2 \quad (13)$$

The final RSS uncertainty was done for the strain- and circumference-based radii (14, 15). The strain, ε, is based on V_g or V_{amp}, resulting in two distinct error values for each radius.

$$\mu_{r_{i_\varepsilon}}^2 = \left(\frac{\partial r_i}{\partial t}\mu_t\right)^2 + \left(\frac{\partial r_i}{\partial d}\mu_d\right)^2 + \left(\frac{\partial r_i}{\partial \varepsilon}\mu_\varepsilon\right)^2 \quad (14)$$

$$\mu_{r_{i_C}}^2 = \frac{\partial r_i}{\partial C}\mu_C \quad (15)$$

References

[1] S. Ridgeway, "Lab 1", Gainesville, FL: 2026, unpublished.
[2] S. Ridgeway, "Lab 1 Introduction", Gainesville, FL: 2026, unpublished.
[3] S. Ridgeway, "Lab 1 Programming", Gainesville, FL: 2026, unpublished.
[4] S. Ridgeway, "Wheatstone Bridge Construction", Gainesville, FL: 2026, unpublished.